Journal of Power Technologies 102 (3) (2022) 88 -- 95

Mathematical analysis of mass and heat transfer through arterial stenosis

Azad Hussain[1*], Lubna Sarwar[1], Sobia Akbar[1], M. Y. Malik[2,3]

[1] Department of Mathematics, University of Gujrat, Gujrat 50700
[2] Dept. of Mathematics, Faculty of Science, King Abdulaziz Univ., P.O. Box 80257, Jeddah 21589, Saudi Arabia
[3] Department of Mathematics, Quaid-I-Azam University, Islamabad 44000, Pakistan
azad.hussain@uog.edu.pk

Abstract

The article investigates the steady state flow of an incompressible fluid which is treated as a Williamson fluid through a stenoised region in the shape of cosine constriction. Blood is taken as a Williamson fluid. Mathematical formulation leads us to nonlinear compatibility and energy equations, which are then deciphered by the shooting technique to obtain the numerical solution. Suitable resemblance transformations are used to change partial differential equations into an embellished form of ordinary differential equations. Further, the consequences of the different parameters involved are shown by graphs and a conclusion is presented. Velocity and temperature fields are canvassed graphically for the distinct values of emerging parameters and discussed in tabular form. Skin friction and the coefficient of heat transfer are also covered in the discussion. The resulting Nusselt number curve exhibits negative deflection for variational values of λ and height of the stenosis δ.

Introduction

Arterial opacity is a widespread medical problem in humans, with atherosclerosis being a leading cause of myocardial infarction and angina. In a coronary artery, occlusion of a partial or total circulatory reduces the supply of blood to the vascular wall and, due to the buildup of plaque with lipid core and a fibrovascular cap, the heart experiences inflexibility and stiffness, which raises the probability of a heart attack. Understanding blood flow in tapered tubes is essential as the taper of the tube is a principal factor in the development of pressure. Arteries may experience narrowing due to the accumulation of substances. These attenuate the artery because blood circulates at high pressure. R. Ellahi et al. [1] studied the flow of blood with suspension of nanoparticles through arterial stenosis. S. Nallapu et al. [2] investigated blood flow in the presence of a magnetic field through narrow tubes. Chemical reaction and heat influences on blood flow through narrow arteries is presented by N. Akbar et al. [3]. Sharma et al. [4] analyzed the Jeffrey-Fluid model of blood flow in tubes. Cheng and Michel [5] studied the flow of non-Newtonian fluids flow through a stenoised channel. Azhar et al. [6] discussed blood flow with transfer of heat in stenosis.

Moreover, in most of the studies, the flow of blood is considered to be Newtonian. The assumption of Newtonian response of blood is for high shear rate flow, i.e., flow through the arteries of large areas. It is not valid when the shear rate is low, as in the flow in arteries of small areas and downstream of the stenosis. In some diseased conditions, blood shows important non-Newtonian properties since experiments proved that mostly biological fluids show non-Newtonian rheology characteristics. The wide range of application of non-Newtonian fluids in industry has attracted much research interest [7–16]. Nadeem and Akbar [17] analyzed the results of variable viscosity in peristaltic Jeffrey-six constant fluid flow in a vertical tube. In non-Newtonian fluids various fluids models are presented, known as second grade fluid, Walters B fluid, PTT fluid, Sisko fluid, Williamson fluid etc. A literature review

revealed that Williamson fluid has been investigated by many researchers over a long period of time.

Motivated by the above-mentioned significance of the fluid and flow geometry, we present our study of steady state flow of a Williamson fluid model through stenosis. The numerical method is used to obtain the governing non-linear system along with boundary conditions. Graphical and tabular results are presented for velocity and temperature fields and discussed in depth. The literature does not seem to contain a single study that deals with the flow of a steady state Williamson fluid model through a stenoised channel. In this exploration, we examine the steady, incompressible flow of a Williamson fluid model through a stenoised region. The introduction is presented in the first section. In the second section governing equations are explained in detail. In section three the physical formulation of the problem is explained. Section four sets out the numerical solution of the presented problem with the assistance of the shooting technique. A discussion about the results of distinct monumental parameters on velocity and temperature fields is given in section five. Concluding remarks on this investigation are presented in the last section.

Governing Equation

The basic governing equations of an incompressible fluid flow are continuity equation, conservation of momentum and energy equation:

$$\vec{\nabla} \cdot \vec{V} = 0 \tag{1}$$

$$\rho \frac{d\vec{V}}{dt} = \vec{\nabla} \cdot \vec{\tau} + \rho b \tag{2}$$

$$\rho c_p \frac{dT}{dt} = k\nabla^2 T + \phi \tag{3}$$

$$\phi = \tau \cdot \nabla V \tag{4}$$

where V is the velocity vector and ρ constant density of fluid b the body force and $\frac{d}{dt}$ material time derivative.

The constitutive equation for Cauchy stress tensor τ for a Williamson fluid is defined as:

$$\tau = -pI + S \tag{5}$$

where

$$S = \begin{bmatrix} s_{xx} & s_{xy} \\ s_{yx} & s_{yy} \end{bmatrix} \tag{6}$$

and p is pressure, I the identity tensor and the constitutive equation for extra stress tensor S is given below:

$$S = \left(\mu_\infty + \frac{(\mu_0 - \mu_\infty)}{1 - \Gamma\dot{\gamma}}\right) A_1 \tag{7}$$

where

$$\dot{\gamma} = \sqrt{\frac{\Pi}{2}}, \qquad \Pi = \frac{1}{2} trac(A_1^2) \tag{8}$$

Problem formulation

In the current problem, the steady state flow of a Williamson fluid through a stenoised region is considered.

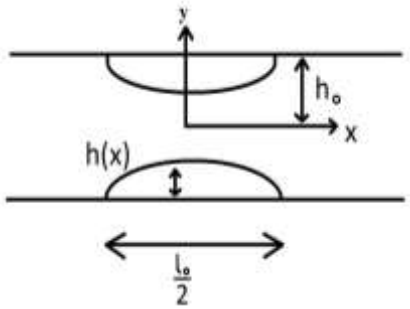

Figure 1: Geometry of the flow problem

For incompressible fluid the continuity equation becomes:

$$\frac{\partial u}{\partial x} + \frac{\partial v}{\partial y} = 0 \tag{9}$$

The governing momentum equation may be expressed as:

$$\rho\left(u\frac{\partial u}{\partial x}+v\frac{\partial u}{\partial y}\right)=-\frac{\partial P}{\partial x}+4\mu_0\frac{\partial^2 u}{\partial x^2}\left(1+\Gamma\sqrt{\left(\frac{\partial u}{\partial x}\right)^2+\frac{1}{2}\left(\frac{\partial u}{\partial y}+\frac{\partial v}{\partial x}\right)^2}\right)+\mu_0\left(1+\Gamma\sqrt{\left(\frac{\partial u}{\partial x}\right)^2+\frac{1}{2}\left(\frac{\partial u}{\partial y}+\frac{\partial v}{\partial x}\right)^2}\right)\times\left(\frac{\partial}{\partial y}\left(\frac{\partial u}{\partial y}+\frac{\partial v}{\partial x}\right)+\frac{\partial^2 u}{\partial y^2}\right) \quad (10)$$

$$\rho\left(u\frac{\partial v}{\partial x}+v\frac{\partial v}{\partial y}\right)=-\frac{\partial P}{\partial y}+\mu_0\frac{\partial}{\partial x}\left(\frac{\partial u}{\partial y}+\frac{\partial v}{\partial x}\right)\left(1+\Gamma\sqrt{\left(\frac{\partial u}{\partial x}\right)^2+\frac{1}{2}\left(\frac{\partial u}{\partial y}+\frac{\partial v}{\partial x}\right)^2}\right) \quad (11)$$

The energy equation takes the form:

$$\rho c_p\left(u\frac{\partial}{\partial x}+v\frac{\partial}{\partial y}\right)T=k\left(\frac{\partial^2}{\partial x^2}+\frac{\partial^2}{\partial y^2}\right)T-p\left(\frac{\partial u}{\partial x}\right)+\mu_0\left(1+\Gamma\sqrt{\left(\frac{\partial u}{\partial x}\right)^2+\frac{1}{2}\left(\frac{\partial u}{\partial y}+\frac{\partial v}{\partial x}\right)^2}\right)\left(2\left(\frac{\partial u}{\partial x}\right)^2+\left(\frac{\partial u}{\partial y}+\frac{\partial v}{\partial x}\right)^2\right) \quad (10)$$

where c_p represents the specific heat of fluid.

Under the above conditions the boundary layer equations for steady incompressible flow toward a stenoised region can be expressed as:

$$u\frac{\partial u}{\partial x}+v\frac{\partial u}{\partial y}=\nu\left(\frac{\partial^2 u}{\partial y^2}\right)\left[1+\frac{\Gamma}{\sqrt{2}}\left(\frac{\partial u}{\partial y}\right)\right] \quad (11)$$

$$-\frac{1}{\rho}\frac{\partial p}{\partial y}=0 \quad (12)$$

$$v\frac{\partial T}{\partial y}=\frac{k}{\rho c_p}\frac{\partial^2 T}{\partial y^2}+\frac{\nu}{c_p}\left[\left(\frac{\partial u}{\partial y}\right)^2+\frac{\Gamma}{\sqrt{2}}\left(\frac{\partial u}{\partial y}\right)^3\right] \quad (13)$$

The proper boundary conditions are:

$$\tilde{u}=\tilde{v}=0,\ \tilde{T}=T_1\ \text{ at } \tilde{y}=h(\tilde{x}),\qquad \frac{\partial\tilde{u}}{\partial\tilde{y}}=0,\quad \frac{\partial\tilde{T}}{\partial\tilde{y}}=0\ \text{ at } \tilde{y}=0 \quad (14)$$

The following relations for u and v are introduced:

$$u=\frac{\partial\psi}{\partial y},\ v=-\delta\frac{\partial\psi}{\partial x}, \quad (15)$$

here ψ is the stream function.

For relations in (13), equation (2) is satisfied automatically and the equations (3—4) take the following form:

$$\frac{\partial\psi}{\partial y}\frac{\partial^2\psi}{\partial x\,\partial y}-\delta\frac{\partial\psi}{\partial x}\frac{\partial^2\psi}{\partial y^2}=\nu\left(\frac{\partial^3\psi}{\partial y^3}\right)\left[1+\frac{\Gamma}{\sqrt{2}}\frac{\partial^2\psi}{\partial y^2}\right]. \quad (16)$$

The boundary conditions reduced to:

$$\psi=\tfrac{1}{2}\text{ at } y=f,\ \psi=0\text{ at } y=0 \quad (17)$$

$$-\delta\frac{\partial\psi}{\partial x}\frac{\partial\tilde{T}}{\partial\tilde{y}}=\frac{k}{\rho C_p}\frac{\partial^2\tilde{T}}{\partial\tilde{y}^2}+\frac{\nu}{c_p}\left[\left(\frac{\partial^2\psi}{\partial y^2}\right)^2+\frac{\Gamma}{\sqrt{2}}\left(\frac{\partial^2\psi}{\partial y^2}\right)^3\right] \quad (18)$$

The dimensionless variable for the stream function is introduced as:

$$\psi=\sqrt{av}xf(\eta) \quad (19)$$

where $\eta = y\frac{\sqrt{a}}{\nu}$ is the similarity variable.

By using equation (14), equations (6—11) finally take the following form:

$$f'''\left(1+\frac{\lambda}{2}f''\right)+\delta f''f-f''f'=0 \quad (20)$$

Next, the non-dimensional temperature θ is shown as:

$$\theta(\eta)=\frac{T-T_0}{T_1-T_0}. \quad (21)$$

Using (17), (20) and the similarity variable, equation (16) reduces to:

$$\theta''+\delta\,\mathrm{Pr}\,\theta'f+\left(1+\frac{\lambda}{2}f''\right)A\theta f''^2=0 \quad (22)$$

where

$$\mathrm{Pr}=\frac{C_p\mu}{k},A=\frac{\mu a^2x^2}{k},\lambda=\Gamma x\sqrt{\frac{2a^3}{\nu}},\nu=\frac{\mu}{\rho} \quad (23)$$

The heat transfer and skin friction coefficient of the flow field are also obtained.

Numerical Solutions

By using the similarity transformations, the governing equations are transformed into ODEs with the cooperation of appropriate conversions. The mathematical result of these equations is found by the implementation of the shooting technique along with the Runge-Kutta method with suitable boundary conditions. Velocity and temperature fields are elaborated to indicate the consequences of the pertinent parameters. The Runge-Kutta method is used to resolve the initial value complications. So, we convert (20) and (22) equalities in first order form

$$f'''=\frac{1}{\left(1+\frac{\lambda}{2}\right)}(-\delta f+f') \quad (24)$$

$$\theta''=-\delta\,\mathrm{Pr}\,\theta'f-\left(1+\frac{\lambda}{2}f''\right)A\theta f''^2 \quad (25)$$

$$f=I_1,\ f'=I_2,\ f''=I_3,\ f'''=I_3',\\ \theta=c_4,\ \theta'=I_5,\ \theta''=I_5' \quad (26)$$

We get the new ordinary differential equations

$$I_1'=I_2,I_2'=I_3,I_4'=I_5 \quad (27)$$

$$I_3'=\frac{1}{\left(1+\frac{\lambda}{2}\right)}(-\delta f+f') \quad (28)$$

$$I_5'=-\delta\,\mathrm{Pr}\,\theta'f-\left(1+\frac{\lambda}{2}f''\right)A\theta f''^2 \quad (29)$$

along with boundary conditions

$$I_1(0)=0,I_2(0)=1,I_2(\infty)=0,\\ I_4(0)=1,I_4(\infty)=0 \quad (30)$$

Results and discussion

To analyze the physics of the problem under consideration, a parametric analysis is carried out and the numerical results are presented with the help of graphs. Figure 1 clearly describes the geometry of the present flow for a better understanding of the problem. Figure 2 indicates the temperature profile for the consequences of A. The temperature profile increases due to the increment in A. Figure 3 illuminates the variations in the temperature field because of δ. It can be seen that by raising δ the temperature profile exhibits lowering behavior. Figure 4 indicates the impact of λ on the temperature profile. The temperature curve goes down by raising λ. Figure 5 clarifies the temperature variations for larger values of Pr. As is expected, for larger values of Pr the temperature shows increasing behavior: Figure 6 reveals the results of λ on the velocity field. It is decreased by the variations of λ. Figure 7 describes the variations in skin friction by varying λ and δ. Figure 8 sets out the consequences of the Nusselt number. It is clear that the curve is bending down gradually. Table. 1 explains the behavior of $\theta'(0)$ at the wall relative to typical dimensionless parameters. Values of $\theta'(0)$ rise through the enhancement in λ, A, Pr and δ. Table. 2 forecasts the impacts of λ and δ on skin friction. When δ and λ increase it can be seen that the values of the skin friction coefficient also rise. Table. 3 clarifies the impact of various parameters on

the heat transfer coefficient. This table indicates the increasing nature of the coefficient due to λ, A, δ and Pr.

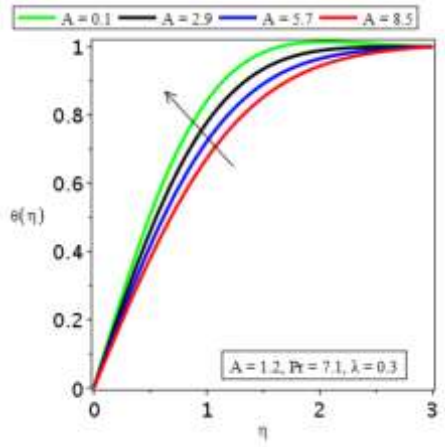

Figure 2: Response of A on the temperature profile

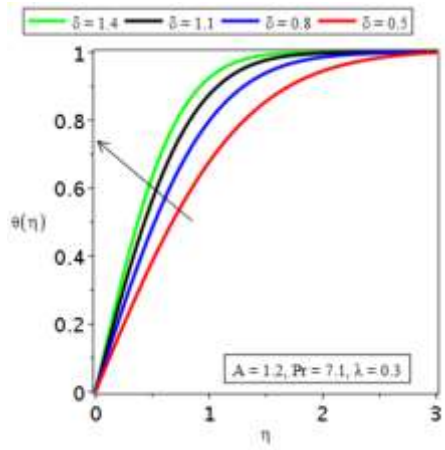

Figure 3: Effects of δ on the temperature field

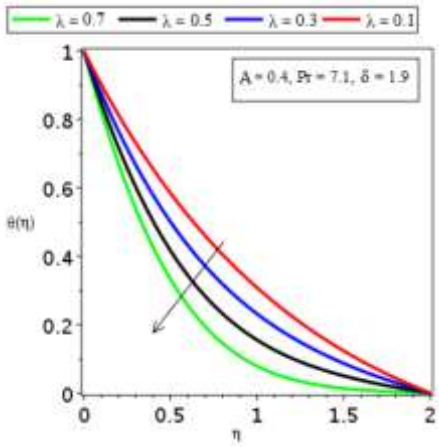

Figure 4: Response of λ on the temperature field

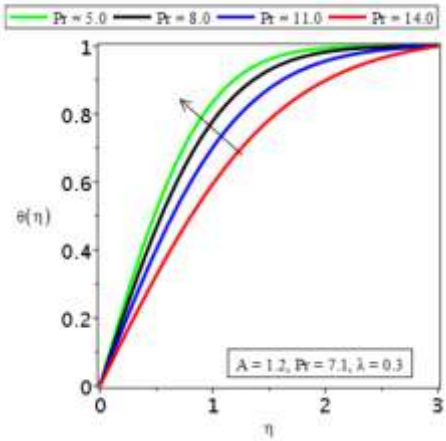

Figure 5: Response of Pr on the temperature field

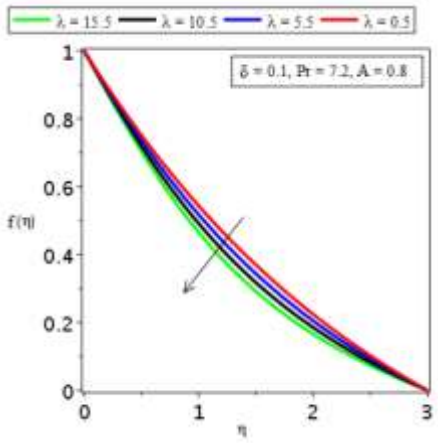

Figure 6: Response of λ on the velocity field

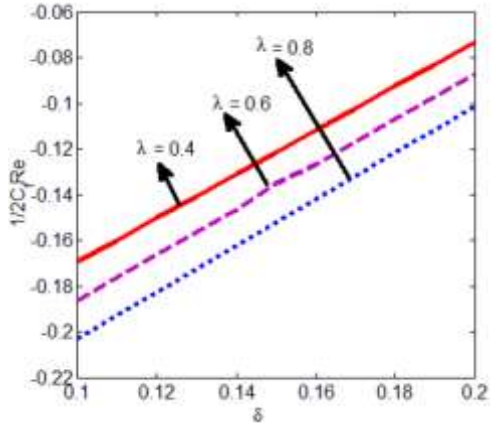

Figure 7: Nusselt number curve for distinct values of λ and δ

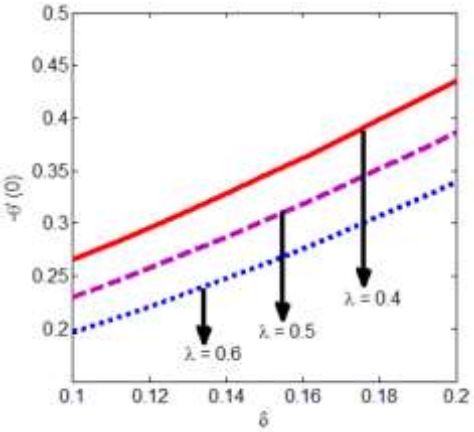

Figure 8: Skin friction curve for λ and δ

Table 1: Values of $\theta'(0)$ at the wall for different parameters

A	0.1	2.9	5.7	8.5
$\lambda = 0.5$				
$\mathrm{Pr} = 7.1$	0.79600	0.88148	0.97995	1.09419
$\delta = 0.53$				

δ	0.5	0.8	1.1	1.4
$Pr = 7.3$				
$\lambda = 0.3$	0.80358	1.04119	1.27328	1.47688
$A = 1.2$				

λ	0.5	0.8	1.1	1.4
$Pr = 7.7$				
$\delta = 3.1$	2.82162	2.83524	2.84999	2.86608
$A = 1.7$				

Pr	7.5	7.8	8.1	9.4
$\delta = 0.5$				
$\lambda = 3.1$	0.67237	0.73968	0.99466	1.12709
$A = 1.6$				

Table 2: Skin friction coefficient values for λ and δ

δ	λ	$\frac{1}{2}C_f\,Re$
0.1	0.1	0.526524
0.11	0.1	0.516157
0.12	0.1	0.505810
0.1	0.1	0.526524
0.1	0.3	0.413206
0.1	0.5	0.424841

Table 3: Values of Nusselt number for δ, A, Pr and λ

δ	A	Pr	λ	$-\theta'(0)$
0.1	0.10	5.0	1.1	0.773294
0.2	0.10	5.0	1.1	1.041918
0.3	0.10	5.0	1.1	1.358806
0.1	0.10	5.0	1.1	0.773294
0.1	0.11	5.0	1.1	1.337216
0.1	0.12	5.0	1.1	1.315871
0.1	0.10	5.0	1.1	1.358806
0.1	0.10	5.2	1.1	1.403354
0.1	0.10	5.3	1.1	1.425837
0.1	0.10	5.0	1.1	1.358806
0.1	0.10	5.0	1.2	1.331089
0.1	0.10	5.0	1.3	1.303561

Concluding Remarks

The flow of blood through stenosis was investigated. Blood was treated as a Williamson fluid. To make a comprehensive study, a scientific model of the problem was constructed including equality of momentum and energy. With the assistance of resemblance transformations, governing equations are transformed into ODEs. A complete graphical study was performed in order to visualize the impact of distinct parameters on temperature and velocity distributions. The significant points of the findings of the current study are as follows:

1. An appreciable excrescence can be seen in the temperature curve due to acceleration in the Prandtl number, A and δ and decreases by increasing the values of λ.
2. Abatement happens in velocity distribution owing to enlargement in λ
3. Skin friction curve shows positive deflection for variational values of λ and δ.
4. Nusselt number curve shows negative deflection for variational values of λ and δ.

References

[1] Ellahi R, Rahman SU, Nadeem S. Blood flow of Jeffrey fluid in a catherized tapered artery with the suspension of nanoparticles. Physics Letters A 2014;378:2973–80. https://doi.org/10.1016/j.physleta.2014.08.002.

[2] Nallapu S, Radhakrishnamacharya G. Jeffrey Fluid Flow through a Narrow Tubes in the Presence of a Magnetic Field. Procedia Engineering 2015;127:185–92. https://doi.org/10.1016/j.proeng.2015.11.325.

[3] Akbar NS, Nadeem S. Influence of heat and chemical reactions on the Sisko fluid model for blood flow through a tapered artery with a mild stenosis. Quaestiones Mathematicae 2014;37:157–77. https://doi.org/10.2989/16073606.2013.779990.

[4] Sharma BD, Yadav PK, Filippov A. A Jeffrey-fluid model of blood flow in tubes with stenosis. Colloid Journal 2017;79:849–56. https://doi.org/10.1134/S1061933X1706014X.

[5] Tu C, Deville M. Pulsatile flow of non-Newtonian fluids through arterial stenoses. Journal of Biomechanics 1996;29:899–908. https://doi.org/10.1016/0021-9290(95)00151-4.

[6] Azhar Mirza, Ali R Ansari, Abdul M Siddiqui, Tahira Haroon. On the steady two-dimensional flow of blood with heat transfer in the presence of a stenosis. WSEAS Transactions on Fluid Mechanics 2013;8:149–58.

[7] Nadeem S, Hussain A, Khan M. HAM solutions for boundary layer flow in the region of the stagnation point towards a stretching sheet.

Communications in Nonlinear Science and Numerical Simulation 2010;15:475–81. https://doi.org/10.1016/j.cnsns.2009.04.037.

[8] Awais M, Malik MY, Bilal S, Salahuddin T, Hussain A. Magnetohydrodynamic (MHD) flow of Sisko fluid near the axisymmetric stagnation point towards a stretching cylinder. Results in Physics 2017;7:49–56. https://doi.org/10.1016/j.rinp.2016.10.016.

[9] Khan I, Malik MY, Hussain A, Salahuddin T. Effect of homogenous-heterogeneous reactions on MHD Prandtl fluid flow over a stretching sheet. Results in Physics 2017;7:4226–31. https://doi.org/10.1016/j.rinp.2017.10.052.

[10] Hussain A, Sarwar L, Nadeem S, Akbar S, Jamal S. Inquisition of combined effects of radiation and MHD on elastico-viscous fluid flow past a pervious plate. Journal of the Brazilian Society of Mechanical Sciences and Engineering 2018;40:343. https://doi.org/10.1007/s40430-018-1228-z.

[11] Hussain A, Malik MY, Bilal S, Awais M, Salahuddin T. Computational analysis of magnetohydrodynamic Sisko fluid flow over a stretching cylinder in the presence of viscous dissipation and temperature dependent thermal conductivity. Results in Physics 2017;7:139–46. https://doi.org/10.1016/j.rinp.2016.12.006.

[12] Malik MY, Hussain A, Nadeem S. Flow of a Non-Newtonian Nanofluid Between Coaxial Cylinders with Variable Viscosity. Zeitschrift Für Naturforschung A 2012;67:255–61. https://doi.org/10.5560/zna.2012-0018.

[13] Hussain A, Sarwar L, Akbar S, Malik MY, Ghafoor S. Model for MHD viscoelastic nanofluid flow with prominence effects of radiation. Heat Transfer-Asian Research 2019;48:463–82. https://doi.org/10.1002/htj.21344.

[14] Hussain A, Ullah A. Boundary layer flow of a Walter's B fluid due to a stretching cylinder with temperature dependent viscosity. Alexandria Engineering Journal 2016;55:3073–80. https://doi.org/10.1016/j.aej.2016.07.037.

[15] Hussain A, Ghafoor S, Malik MY, Jamal S. An exploration of viscosity models in the realm of kinetic theory of liquids originated fluids. Results in Physics 2017;7:2352–60. https://doi.org/10.1016/j.rinp.2017.06.036.

[16] Khan M, Malik MY, Salahuddin T, Khan I. Heat transfer squeezed flow of Carreau fluid over a sensor surface with variable thermal conductivity: A numerical study. Results in Physics 2016;6:940–5. https://doi.org/10.1016/j.rinp.2016.10.024.

[17] Nadeem S, Akbar NS. Effects of temperature dependent viscosity on peristaltic flow of a Jeffrey-six constant fluid in a non-uniform vertical tube. Communications in Nonlinear Science and Numerical Simulation 2010;15:3950–64. https://doi.org/10.1016/j.cnsns.2010.01.019.